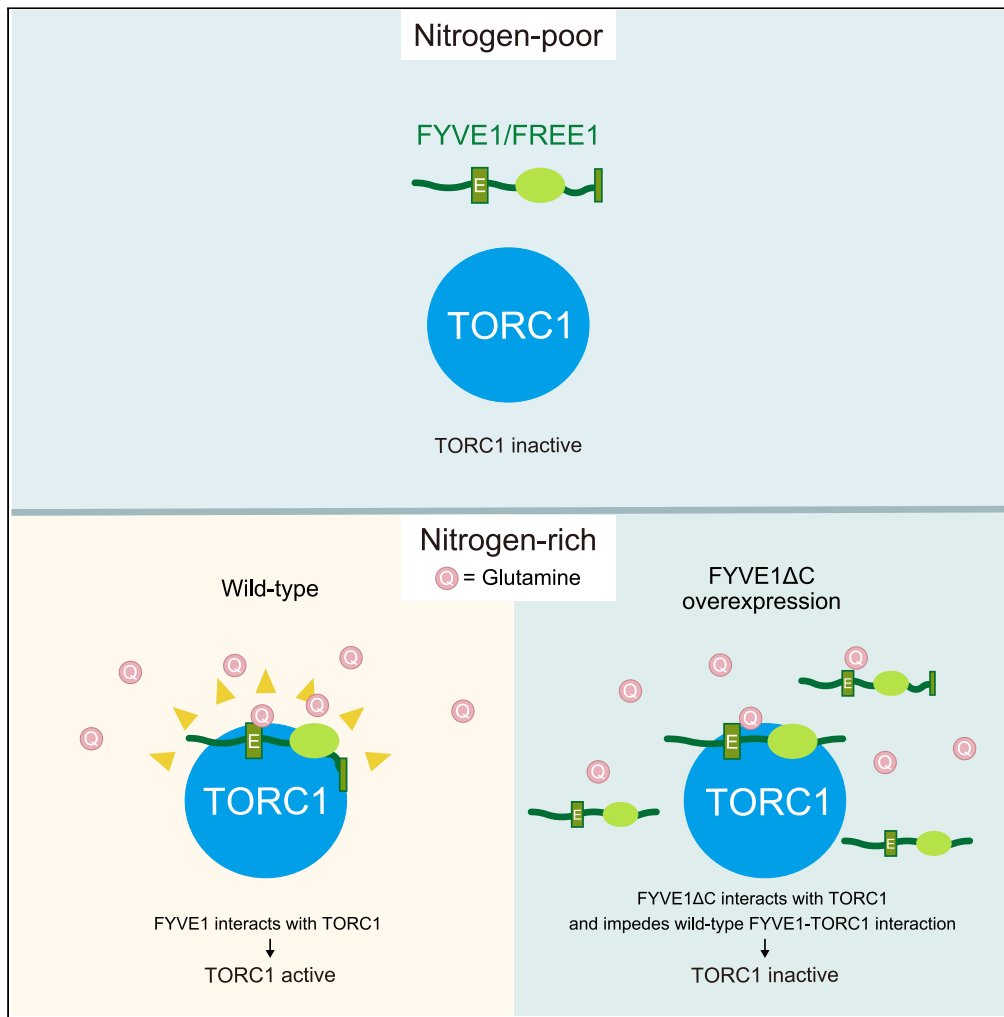


Article

FYVE1/FREE1 is involved in glutamine-responsive TORC1 activation in plants



Mirai Tanigawa,
Tatsuya Maeda,
Erika Isono

tanigawa@hama-med.ac.jp

Highlights

FYVE1 is a plant ortholog of yeast glutamine sensor Pib2

Overexpression of FYVE1ΔC mutant impedes glutamine-responsive TORC1 activation

Glutamine induces FYVE1-TORC1 interaction *in vitro*

FYVE1 is most likely a glutamine sensor that induces TORC1 activation

Tanigawa et al., iScience 27, 110814
September 20, 2024 © 2024
The Author(s). Published by
Elsevier Inc.
<https://doi.org/10.1016/j.isci.2024.110814>



Article

FYVE1/FREE1 is involved
in glutamine-responsive TORC1 activation in plantsMirai Tanigawa,^{1,2,4,*} Tatsuya Maeda,¹ and Erika Isono^{2,3}

SUMMARY

Target of rapamycin complex 1 (TORC1) integrates nutrient availability, growth factors, and stress signals to regulate cellular metabolism according to its environment. Similar to mammals, amino acids have been shown to activate TORC1 in plants. However, as the Rag complex that controls amino acid-responsive TORC1 activation mechanisms in many eukaryotes is not conserved in plants, the amino acid-sensing mechanisms upstream of TORC1 in plants remain unknown. In this study, we report that *Arabidopsis* FYVE1/FREE1 is involved in glutamine-induced TORC1 activation, independent of its previously reported function in ESCRT-dependent processes. FYVE1/FREE1 has a domain structure similar to that of the yeast glutamine sensor Pib2 that directly activates TORC1. Similar to Pib2, FYVE1/FREE1 interacts with TORC1 in response to glutamine. Furthermore, overexpression of a FYVE1/FREE1 variant lacking the presumptive TORC1 activation motif hindered the glutamine-responsive activation of TORC1. Overall, these observations suggest that FYVE1/FREE1 acts as an intracellular amino acid sensor that triggers TORC1 activation in plants.

INTRODUCTION

Controlling the metabolism of living organisms according to their environment is a crucial adaptive mechanism underlying their vital activities. Target of rapamycin complex 1 (TORC1) plays a crucial role in this regulatory process in eukaryotes. TORC1 is activated by growth factors and diverse nutrients, including amino acids, fatty acids, and sugars, and is inhibited by various stresses.^{1–3} Active TORC1 promotes anabolic reactions, such as the synthesis of proteins, nucleic acids, and fatty acids, while concurrently inhibiting catabolic processes such as autophagy, thereby facilitating cell growth.

In mammals and yeast, the mechanisms underlying TORC1 activation by nutrients, particularly amino acids, have been extensively studied in recent years. Amino acids have been shown to activate TORC1 via multiple independent pathways. These include the evolutionarily conserved heterodimeric small GTPases RagA/B-RagC/D (Rag complex) in mammals^{4,5} and Gtr1-Gtr2 (Gtr complex) in yeast.^{6,7} In mammals, several amino acid sensors such as Sestrin2^{8,9} and CASTOR^{10–12} have been identified that function upstream of the Rag complex. Although it has been suggested that intracellular amino acids activate TORC1 also in plants,^{13,14} the Rag complex and its upstream components are absent. To date, a plant-specific small GTPase, ROP2, has been suggested to be involved in amino acid-responsive TORC1 activation, since the expression of a constitutively active ROP2 variant enhances TORC1 activity *in vivo* and ROP2 is activated by the addition of amino acids to the medium.^{14,15} However, the nature of the amino acids or their derivatives that are sensed upstream of TORC1 in plants as well as the underlying molecular mechanism remain still unknown.

Glutamine can activate TORC1 in a Rag pathway-independent manner both in mammals^{16,17} and yeast.¹⁸ In yeast, Pib2 that mainly localizes on the vacuolar membrane is required for Rag-independent TORC1 activation.^{19–23} We recently reported that Pib2 functions not only as an intracellular glutamine sensor but also as a direct TORC1 activator.²⁴ Interestingly, among the proteinogenic amino acids, glutamine has the strongest activation effect on TORC1 in plants,¹⁴ implying that plants have a mechanism to sense intracellular glutamine levels. Therefore, we searched for homologs of Pib2 in *Arabidopsis thaliana* and identified FYVE1/FREE1 as a protein with a domain structure similar to that of Pib2.

FYVE1/FREE1 has previously been reported to function as a plant-specific component of the endosomal sorting complexes required for transport (ESCRT) machinery^{25–27} which is an evolutionarily conserved membrane-remodeling complex essential for plant growth and development. As a component of the ESCRT machinery, FYVE1/FREE1 is crucial for multivesicular endosome (MVE) formation and growth. In addition, FYVE1/FREE1 negatively regulates abscisic acid (ABA) signaling via two mechanisms: first, by degradation of the ABA receptor PYL4 via the endosomal degradation pathway that attenuates ABA response²⁸ and second, by controlling the transcriptional repression of ABA-responsive genes.²⁹ In the latter mechanism, FYVE1/FREE1 is phosphorylated by SnRK2 in an ABA-dependent manner, and the

¹Departments of Biology, Hamamatsu University School of Medicine, Hamamatsu, Shizuoka 431-3125, Japan

²Department of Biology, Faculty of Sciences, University of Konstanz, 78457 Konstanz, Germany

³Division of Molecular Cell Biology, National Institute for Basic Biology, Okazaki 444-8585, Aichi, Japan

⁴Lead contact

*Correspondence: tanigawa@hama-med.ac.jp

<https://doi.org/10.1016/j.isci.2024.110814>



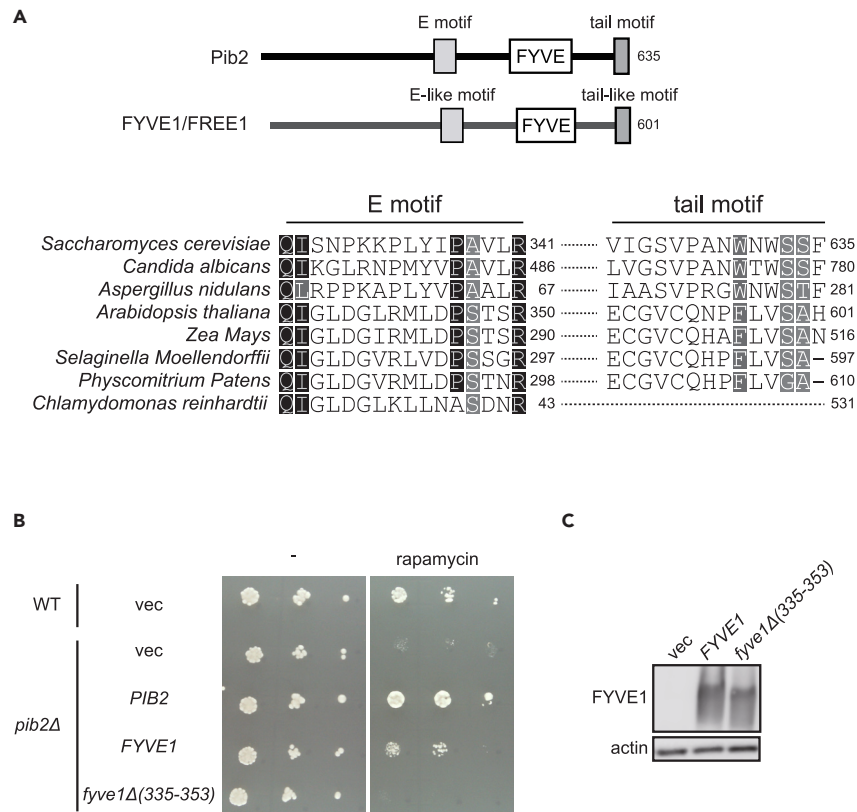


Figure 1. Arabidopsis FYVE1/FREE1 is a possible orthologue of yeast Pib2

(A) Schematic diagram of Pib2 from *Saccharomyces cerevisiae* and FYVE1 from *Arabidopsis thaliana*. Sequence alignments for the indicated species of the Pib2 E and tail motifs are shown below.

(B) Yeast *pib2Δ* phenotype is partially rescued by *Arabidopsis* FYVE1 expression. Yeast wild-type (TM141) or *pib2Δ* (MH1059) strains were transformed with a vector (p425ADH) or plasmids encoding indicated genes (pMH43, pJL59, and pMH517). Serially diluted cell suspensions were spotted on SD medium (supplemented with uracil, tryptophan, and histidine) plates with or without 3.5 nM rapamycin and grown at 30°C for 3 or 4 days, respectively.

(C) Yeast lysates from *pib2Δ* (MH1059) cells carrying a vector (p425ADH) or plasmids encoding indicated genes (pJL59 and pMH517) were subjected to immunoblotting. Actin was used as a loading control. See also Figure S1.

phosphorylated FYVE1/FREE1 translocates into the nucleus to transcriptionally repress ABA-responsive genes. This mechanism is an ESCRT-independent function of FYVE1/FREE1 and forms a negative feedback loop in the ABA signaling pathway. Furthermore, nuclear FYVE1 represses miRNA biogenesis by acting as a negative regulator of the microprocessor machinery involved in the early stages of miRNA processing.³⁰ These observations indicate that FYVE1/FREE1 is a multifunctional protein involved in various cellular processes.

This study reveals an uncharacterized function of FYVE1/FREE1 as a positive regulator of TORC1. FYVE1/FREE1 binds to TORC1 *in vitro* in response to glutamine. Overexpression of a FYVE1/FREE1 mutant variant lacking the C-terminus tail-like motif, which is the presumptive TORC1 activation motif, impedes glutamine-responsive TORC1 activation *in vivo*. Based on these data, we propose a model in which FYVE1/FREE1 senses intracellular glutamine levels to activate TORC1 and mediates nutrient responses in plants.

RESULTS

Arabidopsis FYVE1/FREE1 is a possible yeast Pib2 ortholog

In a previous study, we showed that the yeast vacuolar protein Pib2 functions as a glutamine sensor and directly activates yeast TORC1. To examine whether Pib2 is evolutionarily conserved, we performed a BLAST search and found that FYVE1/FREE1 in *A. thaliana* has a domain structure similar to that of Pib2. The three domains of Pib2 are essential for TORC1 activation. In Pib2, the E motif that binds TORC1, the FYVE domain that interacts with phosphatidylinositol 3-phosphate [PI(3)P] and is responsible for the vacuolar localization of Pib2, and the C-terminal tail motif that contains several conserved aromatic amino acids are essential for TORC1 activation (Figures 1A and S1A).^{19,20,22,24} Similarly, FYVE1 has an E motif-like region (E-like motif) at its center and an FYVE domain between the C-terminus and the E-like motif. The tail motif is not well conserved in FYVE1. However, similar to the Pib2 tail motif, it contains several aromatic amino acids in the C-terminal region (Figure 1A), which we named tail-like motif. Moreover, though the N-terminal halves of FYVE1 and Pib2 lack of sequence homology, both are predicted to be primarily composed of disordered regions (fIDPnn: <http://biomine.cs.vcu.edu/servers/fIDPnn/>).³¹ This prompted us to test

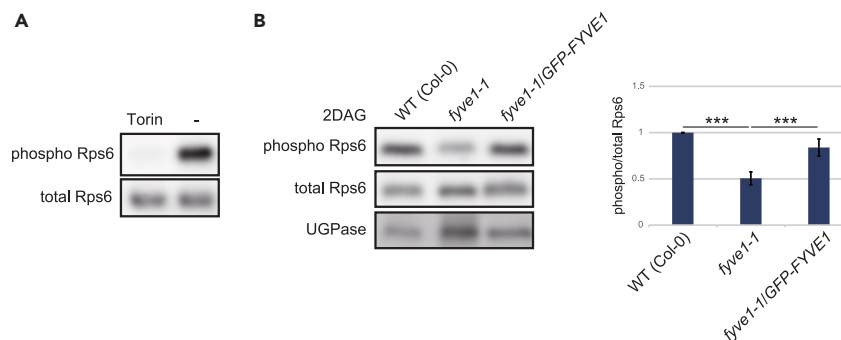


Figure 2. TORC1 activity is reduced in the *fyve1-1* mutant

(A) Monitoring TORC1 activity based on Ser240 phosphorylation of RPS6. Wild-type Arabidopsis seedlings 2 days after germination were treated with 25 μ M of Torin 2 for 1 h, and the total extracts were subjected to immunoblotting using anti-phospho-Ser240-RPS6-specific and anti-RPS6 antibodies.

(B) TORC1 activity is reduced in the *fyve1-1* mutant. Total extracts from seedlings of indicated lines were subjected to immunoblot as in (A). UGPase was used as a loading control. The bar graph shows ratio of phosphorylated/total Rps6 normalized to the values of wild-type (Col-0). Error bars represent the standard deviation ($n = 3$ independent experiments), and significance was determined using a two-tailed Student's *t* test. Statistically significant differences are indicated with asterisks (***) representing $p < 0.001$.

whether FYVE1 is a Pib2 ortholog. At first, we examined whether the exogenous expression of *FYVE1* in yeast complements the rapamycin sensitivity of yeast *pib2 Δ* cells. *pib2 Δ* cells exhibit reduced growth in media supplemented with rapamycin.^{19,20,22} The phenotype was partially rescued by the expression of *FYVE1* (Figure 1B). In contrast, *FYVE1* Δ 335-353, which lacks the E-like motif, failed to rescue the rapamycin sensitivity of *pib2 Δ* even though its expression was comparable to wild-type *FYVE1* (Figures 1B and 1C). As the Pib2 E motif is responsible for the interaction with TORC1, FYVE1 may interact with TORC1 through its E-like motif.

TORC1 activity is reduced in the *fyve1-1* mutant

To test whether FYVE1 functions as a positive regulator of TORC1 similar to Pib2, we monitored TORC1 activity in the *fyve1-1* mutant (pst18264 RIKEN), which carries a Ds transposon in the first exon of the *FYVE1* gene.^{27,32} To examine TORC1 activity in Arabidopsis seedlings, we monitored the phosphorylation of RPS6 at Ser240 that is phosphorylated by S6K upon activation by TORC1. We confirmed that the phosphorylation of RPS6 at Ser240 reflects TORC1 activity as reported previously,³³ as Torin 2 treatment that selectively inhibits TOR activity diminished the phosphorylation (Figure 2A). Expectedly, in the *fyve1-1* mutant, TORC1 activity was significantly reduced compared to that in the wild-type and *GFP-FYVE1* complemented lines (Figure 2B), suggesting that FYVE1 is necessary for intact TORC1 activation.

Overexpression of a *fyve1* Δ C mutant impedes glutamine-responsive TORC1 activation

fyve1-1 causes seedling lethality, most probably due to the role of FYVE1 in ESCRT-mediated processes essential for plant growth, making it challenging to perform biochemical experiments with the *fyve1-1* mutant. Therefore, we attempted an alternative approach using a dominant-negative *FYVE1* mutant. In yeast, overexpression of a *pib2* variant lacking the C-terminal tail motif (*pib2 Δ 621-635*) causes severe growth defects (data not shown). The dominant-negative phenotype of the mutant is canceled by the R341A mutation in the E motif, which impairs the TORC1 binding ability.²⁴ These observations indicate that the dominant negative effect of *pib2 Δ 621-635* is caused by binding to TORC1 but not being able to activate TORC1. Analogously, if FYVE1 binds to TORC1 via the E-like motif and activates TORC1 via the C-terminal tail-like motif, then overexpression of C-terminal truncation of FYVE1 is expected to inhibit TORC1 activation. To test this idea, transgenic plants overexpressing *FYVE1* Δ 582-601 (*FYVE1* Δ C) under the cauliflower mosaic virus 35S promoter were generated and the effect of the overexpression on TORC1 was evaluated. Glutamine addition to the medium induced TORC1 activation in wild-type (Col-0) and wild-type *FYVE1* overexpressing plants. In contrast, glutamine-dependent activation was diminished in *FYVE1* Δ C overexpressing plants (Figures 3A and 3B).

FYVE1 was reported to be degraded by autophagy and proteasomes under stress conditions.^{34,35} We observed that the FYVE1 levels increased in response to glutamine treatment (Figure 3A), which was not due to elevated *FYVE1* mRNA level (Figure S2). We also observed a decrease in FYVE1 protein levels upon treatment with Torin 2 (Figure S3), suggesting autophagy inhibition by activated TORC1 could impact FYVE1 stability.

In cell culture-derived protoplasts, overexpression of *FYVE1* Δ C inhibited the glutamine-responsive TORC1 activation (Figures 3C and 3D). Furthermore, the dominant negative effect of *FYVE1* Δ C overexpression in the protoplasts was canceled by simultaneous deletion of the E-like motif (Δ 335-350 = Δ E) (Figures 3C and 3D), suggesting that *FYVE1* Δ C inhibits the glutamine-responsive TORC1 activation through direct TORC1 interaction via its E-like motif.

To test the effect of FYVE1 overexpression on plant growth, we compared root growth in lines overexpressing wild-type *FYVE1* and the *FYVE1* Δ C mutant to the same extent. The root growth of the *FYVE1* Δ C overexpressing line was inhibited on nitrogen-containing medium without (+N–G) and with (+N+G) glucose (Figures 3E and 3F). The growth of the wild-type *FYVE1* overexpressing line was also slightly

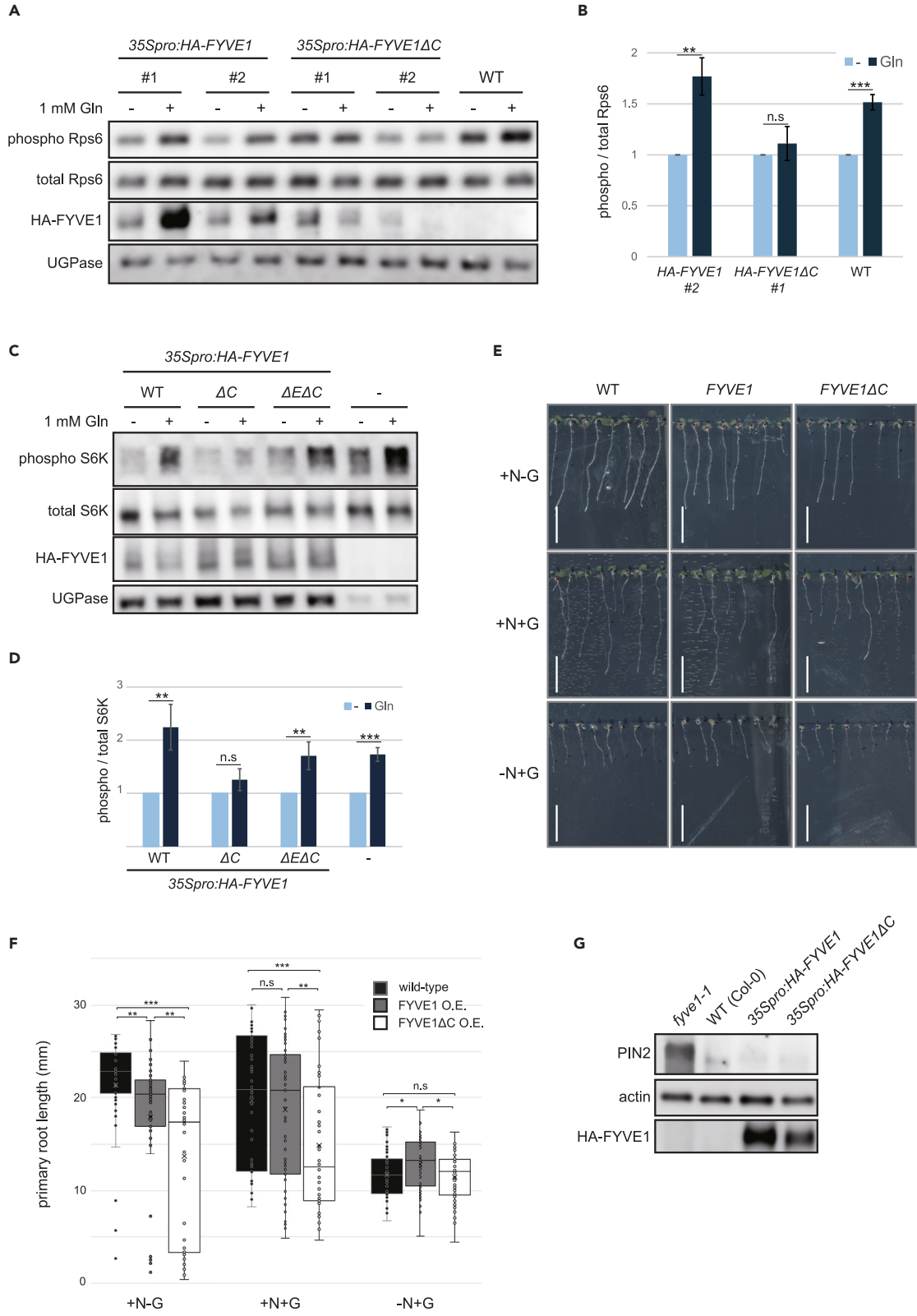


Figure 3. Overexpression of FYVE1ΔC mutant impedes glutamine-responsive TORC1 activation

(A and B) *35Spro:HA-FYVE1* and *35Spro:HA-FYVE1ΔC* transgenic seedlings were treated with 1 mM L-glutamine for 20 min, and the total extracts were subjected to immunoblotting. UGPase was used as a loading control. The ratio of phosphorylated/total Rps6, normalized to the values for each line to which glutamine was not added, is shown for representative lines in B). Error bars represent the standard deviation ($n = 3$ independent experiments), and significance was determined by a two-tailed Student's *t* test. Statistically significant differences are indicated with asterisks, (**) representing $p < 0.01$ and (***) representing $p < 0.001$.

(C and D) Root-cultured cell derived protoplasts transformed with plasmids harboring both *35Spro:S6K* and indicated *35Spro:FYVE1* mutants were treated with 1 mM L-glutamine for 10 min, and the total extracts were subjected to immunoblotting. The ratio of phosphorylated/total S6K normalized to the values for each transformant to which glutamine was not added in D). Error bars represent the standard deviation ($n = 3$ independent experiments). Significance was determined by a two-tailed Student's *t* test. Statistically significant differences are indicated with (**) representing $p < 0.01$ and (***) representing $p < 0.001$.

(E) Photographs of wild-type, *35Spro:HA-FYVE1*, and *35Spro:HA-FYVE1ΔC* seedlings grown for 7-day on 1/2 MS (+N–G), 1/4 MS with glucose (+N+G), and grown for 9 days on 1/4 MS without nitrogen but with glucose (–N+G). Scale bars: 1 cm.

(F) Boxplots of primary root length of 7-day-old seedlings grown on 1/2 MS (+N–G), 1/4 MS with glucose (+N+G), and of 9-day-old seedlings grown on 1/4 MS without nitrogen but with glucose (–N+G) tested for wild-type ($n = 55, 57,$ and 57 seedlings, respectively), *35Spro:HA-FYVE1* ($n = 55, 55,$ and 54 seedlings, respectively), and *35Spro:HA-FYVE1ΔC* ($n = 53, 52,$ and 52 seedlings, respectively). Error bars represent standard deviation among the independent samples and the cross and the horizontal lines in each box represent mean and median values, respectively. Statistically significant differences between the lines are indicated with asterisk (*) representing $p < 0.05$, (**) representing $p < 0.01$, and (***) representing $p < 0.001$, based on a two-tail *t* test assuming unequal variance between the lines.

(G) PIN2 levels in seedlings of wild-type (Col-0) and indicated transgenic lines. Total extracts were subjected to immunoblotting with anti-PIN2 antibody. Actin was used as a loading control. See also Figures S2, S3, and S4.

inhibited on nitrogen-containing medium; however, the phenotype was milder than that of the *FYVE1ΔC* mutant line (Figures 3E and 3F). In contrast, on a nitrogen-free medium with glucose (–N+G), the *FYVE1ΔC* overexpression line did not show significant differences with wild-type seedlings (Figures 3E and 3F). The difference in phenotypic severity was probably because TORC1 was already largely inactivated under nitrogen starvation and *FYVE1ΔC* overexpression did not further reduce TORC1 activity.

As FYVE1 interacts with multiple components of the ESCRT machinery, the dominant-negative effect of *FYVE1ΔC* could be caused by the inhibition of ESCRT function.^{25,26,36} To examine ESCRT functions in *FYVE1ΔC* overexpressing plants, we monitored PIN2 protein levels, which is sorted into MVE and degraded in the vacuolar lumen.^{37,38} While PIN2 accumulated in *fyve1-1* seedlings as previously reported,²⁵ apparent differences were not observed between wild-type (Col-0), wild-type *FYVE1*, and *FYVE1ΔC* overexpressing plants (Figure 3G). Similarly, *fyve1-1* mutant seedlings and PI3K- and PI4K inhibitor wortmannin-treated wild-type seedlings showed accumulation of ubiquitylated proteins as previously reported.^{25,27,39} In contrast, the amounts of ubiquitylated proteins in *FYVE1* and *FYVE1ΔC* overexpression lines were comparable to those in the wild-type (Figure S4). These data suggest that ESCRT- and ubiquitin-mediated endosomal degradation is retained in *FYVE1ΔC* overexpressing plants and that the impairment of glutamine-responsive TORC1 activation in the *FYVE1ΔC* overexpressing plants is not due to ESCRT dysfunction.

L-glutamine induces FYVE1-TORC1 interaction in vitro

In yeast, Pib2 binds directly to TORC1 in response to glutamine and activates TORC1.²⁴ Mass spectrometry (MS) data using FYVE1 as bait identified TORC1 components Lst8-2 and Raptor1B as potential interactors of FYVE1³⁶. To test the interaction between FYVE1 and TORC1 *in vitro*, we generated HA-tagged *LST8-2* and *RAPTOR1B* overexpressing lines. Since we could not detect HA-Raptor1B but not HA-Lst8-2 in the obtained lines by western blotting, we performed an *in vitro* pull-down assay using HA-Raptor1B overexpressing lines. GST-FYVE1 purified from *E. coli* was incubated with plant lysates from HA-Raptor overexpressing lines. HA-Raptor was co-precipitated with GST-FYVE1, and this interaction was enhanced by the addition of L-glutamine to the lysates (Figure 4A). To induce the maximum binding, millimolar levels of glutamine were required, which is within the range of the intracellular glutamine level in Arabidopsis cells (Figure 4B).⁴⁰ Furthermore, the glutamine-responsive TORC1 interaction was abolished in the *FYVE1ΔE* mutant (Figure 4C), suggesting that the E-like motif is necessary for the glutamine-responsive binding to TORC1. Notably, FYVE1-TORC1 interaction was increased only by L-glutamine, but not by other tested amino acids including L-cysteine, which induced Pib2-TORC1 interaction^{24,41} (Figure 4A).

Altogether, our results identified Arabidopsis FYVE1 as an ortholog of yeast Pib2 that can act as a glutamine sensor. TORC1 activation by FYVE1 was dependent on the C-terminal tail-like motif and this function of FYVE1 is likely ESCRT-independent. Given the amino acid identity of FYVE1 and its homologs in other plant species (Figure 1A), it can be expected that FYVE1 function is conserved in plants. Thus, we propose that FYVE1 is a positive regulator of TORC1 in plants, and increasing FYVE1 levels under favorable conditions and conversely decreasing them under stress conditions could be part of a feedback mechanism during nutrient response in plants (Figure 5).

DISCUSSION

This study identifies FYVE1/FREE1 as a positive regulator of TORC1 in *A. thaliana*. Overall, our experiments indicate that FYVE1 is the plant Pib2 ortholog and suggest that FYVE1 is an intracellular glutamine sensor that triggers TORC1 activation.

Pib2 has been recently reported to function also as a cysteine sensor in yeast.⁴¹ While the binding of Pib2 to TORC1 is induced by cysteine and glutamine,^{24,41} the binding of FYVE1 to TORC1 was not induced by cysteine, suggesting that FYVE1 does not function as a cysteine sensor. In plants also, cysteine has been suggested to activate TORC1,^{14,42} although the activation mechanism is probably independent of FYVE1.

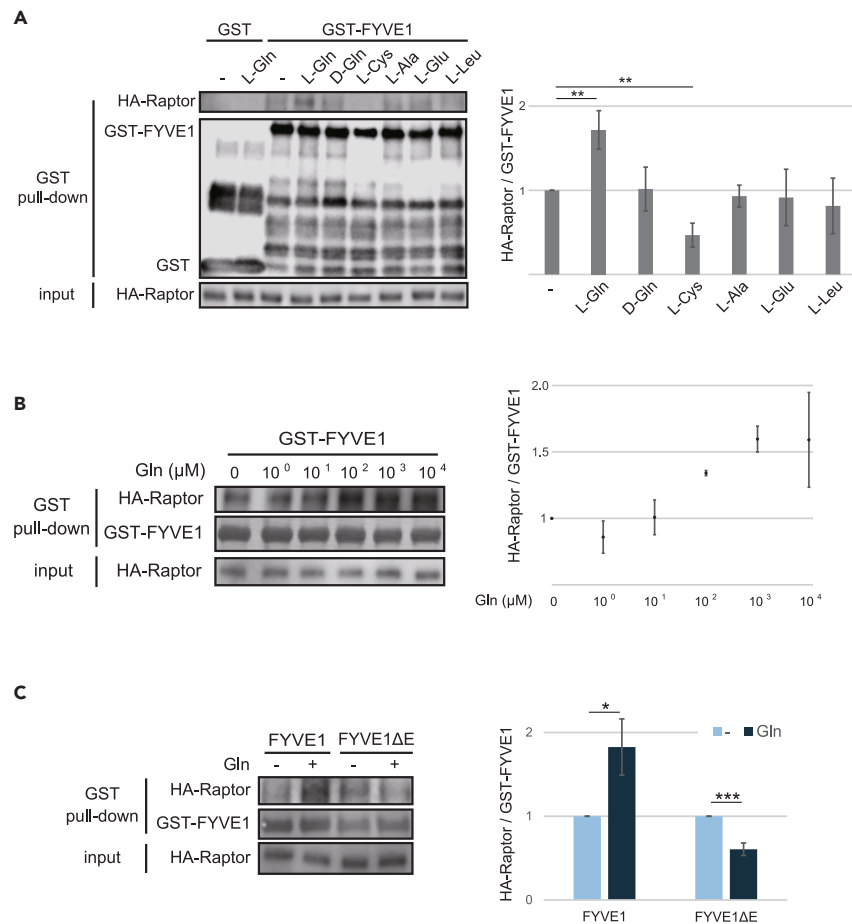


Figure 4. L-glutamine induces FYVE1-TORC1 interaction in vitro

(A) L-glutamine specifically induces FYVE1-TORC1 interaction. Plant cell lysates from HA-Raptor1B expressing seedlings were subjected to pull-down assays with bacterially expressed GST-FYVE1 and the final 1 mM of indicated amino acids. The bar graph shows GST-FYVE1-bound HA-Raptor1B normalized to the samples without amino acids. Error bars represent the standard deviation ($n = 3$ independent experiments). Significance was determined using a two-tailed Student's *t* test. Statistically significant differences are indicated with asterisks (**) representing $p < 0.01$.

(B) The FYVE1-TORC1 interaction depends on glutamine concentration. Pull-down assays were performed as in (A), except that the indicated concentrations of L-glutamine were added to the cell lysates. Dot plots represent the ratio of GST-FYVE1-bound HA-Raptor1B normalized to the samples without glutamine. Error bars represent the standard deviation ($n = 3$ independent experiments).

(C) The E-like motif of FYVE1 is required for the glutamine-induced FYVE1-TORC1 interaction. Pull-down assays were performed as in (A) using GST-FYVE1 or GST-FYVE1ΔE(Δ335-350). The bar graph shows GST-FYVE1- or FYVE1ΔE-bound HA-Raptor1B normalized to the samples without glutamine. Error bars represent the standard deviation ($n = 3$ independent experiments). Statistically significant differences are indicated with asterisks (*) representing $p < 0.05$ and (***) representing $p < 0.001$.

It is noteworthy that both Pib2 and FYVE1 are phosphorylated and regulated by stress-activated AMP-activated protein kinase (AMPK) orthologs. In *Arabidopsis*, when nutrients are depleted, FYVE1 is phosphorylated by the AMPK ortholog SnRK1α1, thereby being recruited to the autophagosome membrane where it plays an essential role in autophagosome closure by probably bridging the ATG conjugation system and ESCRT machinery.³⁶ In yeast, Pib2 is phosphorylated by the AMPK ortholog Snf1 to inhibit the Pib2-TORC1 interaction under energy-depleted conditions.⁴³ In other words, Pib2 and FYVE are signaling hubs that function downstream of AMPK and upstream of TORC1, depending on the environment. Given the mutually inhibitory relationship between AMPK and TORC1, factors upstream of one signal being regulated downstream of the other might be a natural evolutionary consequence.

Is Pib2 evolutionarily conserved across animal species? Mammals have LAPF/phafin1, which has an FYVE domain and C-terminal sequence that are homologous to the tail motif of Pib2 (Figure S1A).¹⁹ However, it was reported that knockdown of LAPF/phafin1 in RagA/B knockout cells did not affect the glutamine-responsive TORC1 activation,⁴⁴ and to date, no clear phenotype of LAPF/phafin1 knockdown or knockout in TORC1 signaling has been reported. Notably, the C-termini of LAPF/phafin1 homologs in flies and nematodes lack homology with the tail motif of Pib2 (Figure S1B), implying that these homologs, including LAPF/phafin1, may have lost their function as TORC1 activators during evolution.

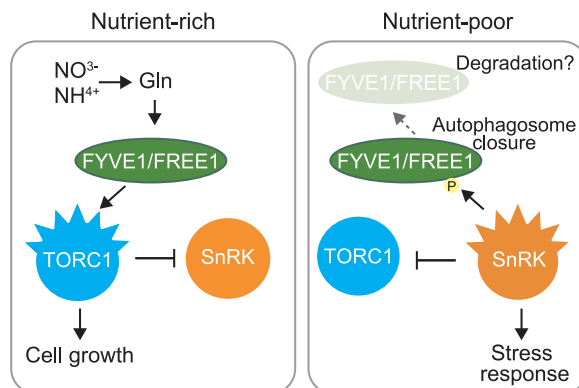


Figure 5. Model of the roles of FYVE1 in the nutrient response

Under nutrient-rich conditions, FYVE1 is activated by glutamine and interacts with TORC1, leading to TORC1 activation. Under nutrient-poor conditions, FYVE1 is phosphorylated by active SnRK1, thereby being recruited to autophagosomes, where it promotes autophagosome closure and probably its own degradation.

What could be the advantage of sensing glutamine upstream of TORC1? As yeast and plants can synthesize all proteinogenic amino acids on their own and, unlike mammals, probably do not have amino acids that could bottleneck their growth. Therefore, monitoring the amount of nitrogen stored in cells is a low-cost strategy for the cell compared to monitoring the amounts of individual amino acids in the cells. Here, glutamine has properties that make it suitable as an indicator of the amounts of intracellular nitrogen storage. First, glutamine, which has two amino groups per molecule, is one of the most abundant free amino acids in both yeast and plants,^{40,45} indicating that glutamine occupies a large mass of nitrogen in cells. Second, intracellular glutamine levels reliably reflect the nitrogen status of cells. Under nitrogen starvation conditions, the intracellular glutamine level decreases to <5% within 30 min after starvation in yeast cells, whereas the level of glutamate, which can be generated by glutamine deamination, remains at approximately 40%.⁴⁶ As glutamate is at a metabolic crossroads with other amino acids and metabolites, maintaining a stable glutamate level is probably crucial for maintaining cellular homeostasis. Therefore, glutamine possibly functions as a nitrogen storage molecule for this purpose and is perceived as an indicator of nitrogen storage.

Limitations of the study

Although we showed that L-glutamine induces the FYVE1-TORC1 interaction *in vitro*, how FYVE1 functions as a sensor *in vivo* and whether FYVE1 directly activates TORC1, such as Pib2, remain unclear. Future studies should address these questions.

RESOURCE AVAILABILITY

Lead contact

Further information and requests for resources and reagents should be directed to and will be fulfilled by the lead contact, Mirai Tanigawa (tanigawa@hama-med.ac.jp).

Materials availability

Materials generated in this study are available from the [lead contact](#) upon reasonable request.

Data and code availability

- Original western blot images and plant photos have been deposited at Mendeley Data and are publicly available as of the date of publication. The DOI is listed in the [key resources table](#).
- This paper does not report original code.
- Any additional information required to reanalyze the data reported in this paper is available from the [lead contact](#) upon request.

ACKNOWLEDGMENTS

We thank M.K. Nagel and all members of the Isono lab for supporting M.T. in performing the Arabidopsis experiments. We also thank all members of the Maeda lab, especially M. Toyama for technical assistance. We appreciate the members of the Tokai Tor Conference (ToToCo) for general discussions. This work was supported by JSPS KAKENHI grant Numbers 20K06555 and 21KK0265 (to M.T.), 20H03251 and 23H02142 (to T.M.), HUSM Grant-in-Aid (to T.M.), and SFB 969 (to E.I.).

AUTHOR CONTRIBUTIONS

Conceptualization, M.T., T.M., and E.I.; methodology, M.T., T.M., and E.I.; investigation, M.T.; writing – original draft, M.T.; writing – review & editing, M.T., T.M., and E.I.; funding acquisition, M.T.; supervision, T.M. and E.I.

DECLARATION OF INTERESTS

The authors declare no competing interests.

STAR★METHODS

Detailed methods are provided in the online version of this paper and include the following:

- **KEY RESOURCES TABLE**
- **EXPERIMENTAL MODEL AND STUDY PARTICIPANT DETAILS**
 - Yeast strains and growth conditions
 - Plant material and growth conditions
- **METHOD DETAILS**
 - Monitoring TOR kinase activity in seedlings
 - Monitoring TOR kinase activity in protoplasts
 - GST-FYVE1 purification from *E. coli*
 - *In vitro* pull-down assay
 - qRT-PCR
- **QUANTIFICATION AND STATISTICAL ANALYSIS**

SUPPLEMENTAL INFORMATION

Supplemental information can be found online at <https://doi.org/10.1016/j.isci.2024.110814>.

Received: April 9, 2024

Revised: July 6, 2024

Accepted: August 22, 2024

Published: August 26, 2024

REFERENCES

1. Saxton, R.A., and Sabatini, D.M. (2017). mTOR signaling in growth, metabolism, and disease. *Cell* 168, 960–976. <https://doi.org/10.1016/j.cell.2017.02.004>.
2. González, A., and Hall, M.N. (2017). Nutrient sensing and TOR signaling in yeast and mammals. *EMBO J.* 36, 397–408. <https://doi.org/10.15252/embj.20169610>.
3. Goul, C., Peruzzo, R., and Zoncu, R. (2023). The molecular basis of nutrient sensing and signalling by mTORC1 in metabolism regulation and disease. *Nat. Rev. Mol. Cell Biol.* 24, 857–875. <https://doi.org/10.1038/s41580-023-00641-8>.
4. Sancak, Y., Peterson, T.R., Shaul, Y.D., Lindquist, R.A., Thoreen, C.C., Bar-Peled, L., and Sabatini, D.M. (2008). The Rag GTPases bind raptor and mediate amino acid signaling to mTORC1. *Science* 320, 1496–1501. <https://doi.org/10.1126/science.1157535>.
5. Sancak, Y., Bar-Peled, L., Zoncu, R., Markhard, A.L., Nada, S., and Sabatini, D.M. (2010). Regulator-Rag complex targets mTORC1 to the lysosomal surface and is necessary for its activation by amino acids. *Cell* 141, 290–303. <https://doi.org/10.1016/j.cell.2010.02.024>.
6. Binda, M., Péli-Gulli, M.P., Bonfils, G., Panchaud, N., Urban, J., Sturgill, T.W., Loewith, R., and De Virgilio, C. (2009). The Vam6 GEF controls TORC1 by activating the EGO complex. *Mol. Cell.* 35, 563–573. <https://doi.org/10.1016/j.molcel.2009.06.033>.
7. Panchaud, N., Péli-Gulli, M.P., and De Virgilio, C. (2013). Amino acid deprivation inhibits TORC1 through a GTPase-activating protein complex for the Rag family GTPase Gtr1. *Sci. Signal.* 6, ra42. <https://doi.org/10.1126/scisignal.2004112>.
8. Wolfson, R.L., Chantranupong, L., Saxton, R.A., Shen, K., Scaria, S.M., Cantor, J.R., and Sabatini, D.M. (2016). Sestrin2 is a leucine sensor for the mTORC1 pathway. *Science* 351, 43–48. <https://doi.org/10.1126/science.aab2674>.
9. Saxton, R.A., Knockenhauer, K.E., Wolfson, R.L., Chantranupong, L., Pacold, M.E., Wang, T., Schwartz, T.U., and Sabatini, D.M. (2016). Structural basis for leucine sensing by the Sestrin2-mTORC1 pathway. *Science* 351, 53–58. <https://doi.org/10.1126/science.aad2087>.
10. Chantranupong, L., Scaria, S.M., Saxton, R.A., Gygi, M.P., Shen, K., Wyant, G.A., Wang, T., Harper, J.W., Gygi, S.P., and Sabatini, D.M. (2016). The CASTOR proteins are arginine sensors for the mTORC1 pathway. *Cell* 165, 153–164. <https://doi.org/10.1016/j.cell.2016.02.035>.
11. Saxton, R.A., Chantranupong, L., Knockenhauer, K.E., Schwartz, T.U., and Sabatini, D.M. (2016). Mechanism of arginine sensing by CASTOR1 upstream of mTORC1. *Nature* 536, 229–233. <https://doi.org/10.1038/nature19079>.
12. Zhou, Y., Wang, C., Xiao, Q., and Guo, L. (2019). Crystal structures of arginine sensor CASTOR1 in arginine-bound and ligand free states. *Biochem. Biophys. Res. Commun.* 508, 387–391. <https://doi.org/10.1016/j.bbrc.2018.11.147>.
13. Cao, P., Kim, S.J., Xing, A., Schenck, C.A., Liu, L., Jiang, N., Wang, J., Last, R.L., and Brandizzi, F. (2019). Homeostasis of branched-chain amino acids is critical for the activity of TOR signaling in Arabidopsis. *Elife* 8, e50747. <https://doi.org/10.7554/eLife.50747>.
14. Liu, Y., Duan, X., Zhao, X., Ding, W., Wang, Y., and Xiong, Y. (2021). Diverse nitrogen signals activate convergent ROP2-TOR signaling in Arabidopsis. *Dev. Cell* 56, 1283–1295.e5. <https://doi.org/10.1016/j.devcel.2021.03.022>.
15. Schepetilnikov, M., Makarian, J., Srour, O., Geldreich, A., Yang, Z., Chicher, J., Hammann, P., and Ryabova, L.A. (2017). GTPase ROP2 binds and promotes activation of target of rapamycin, TOR, in response to auxin. *EMBO J.* 36, 886–903. <https://doi.org/10.15252/embj.201694816>.
16. Thomas, J.D., Zhang, Y.J., Wei, Y.H., Cho, J.H., Morris, L.E., Wang, H.Y., and Zheng, X.F.S. (2014). Rab1A is an mTORC1 activator and a colorectal oncogene. *Cancer Cell* 26, 754–769. <https://doi.org/10.1016/j.ccell.2014.09.008>.
17. Jewell, J.L., Kim, Y.C., Russell, R.C., Yu, F.X., Park, H.W., Plouffe, S.W., Tagliabracci, V.S., and Guan, K.L. (2015). Differential regulation of mTORC1 by leucine and glutamine. *Science* 347, 194–198. <https://doi.org/10.1126/science.1259472>.
18. Stracka, D., Jozefczuk, S., Rudroff, F., Sauer, U., and Hall, M.N. (2014). Nitrogen source activates TOR (Target of Rapamycin) complex 1 via glutamine and independently of Gtr/Rag proteins. *J. Biol. Chem.* 289, 25010–25020. <https://doi.org/10.1074/jbc.M114.574335>.
19. Kim, A., and Cunningham, K.W. (2015). A LAPF/phafin1-like protein regulates TORC1 and lysosomal membrane permeabilization in response to endoplasmic reticulum membrane stress. *Mol. Biol. Cell* 26, 4631–4645. <https://doi.org/10.1091/mbc.E15-08-0581>.
20. Michel, A.H., Hatakeyama, R., Kimmig, P., Arter, M., Peter, M., Matos, J., De Virgilio, C., and Kornmann, B. (2017). Functional mapping of yeast genomes by saturated transposition. *Elife* 6, e23570. <https://doi.org/10.7554/eLife.23570>.
21. Tanigawa, M., and Maeda, T. (2017). An in vitro TORC1 kinase assay that recapitulates the Gtr-independent glutamine-responsive TORC1 activation mechanism on yeast vacuoles. *Mol. Cell Biol.* 37, e00075-17. <https://doi.org/10.1128/MCB.00075-17>.
22. Ukai, H., Araki, Y., Kira, S., Oikawa, Y., May, A.I., and Noda, T. (2018). Gtr/Ego-independent

- TORC1 activation is achieved through a glutamine-sensitive interaction with Pib2 on the vacuolar membrane. *PLoS Genet.* 14, e1007334. <https://doi.org/10.1371/journal.pgen.1007334>.
23. Hatakeyama, R. (2021). Pib2 as an emerging master regulator of yeast TORC1. *Biomolecules* 11, 1489. <https://doi.org/10.3390/biom11101489>.
 24. Tanigawa, M., Yamamoto, K., Nagatoishi, S., Nagata, K., Noshiro, D., Noda, N.N., Tsumoto, K., and Maeda, T. (2021). A glutamine sensor that directly activates TORC1. *Commun. Biol.* 4, 1093. <https://doi.org/10.1038/s42003-021-02625-w>.
 25. Gao, C., Luo, M., Zhao, Q., Yang, R., Cui, Y., Zeng, Y., Xia, J., and Jiang, L. (2014). A Unique plant ESCRT component, FREE1, regulates multivesicular body protein sorting and plant growth. *Curr. Biol.* 24, 2556–2563. <https://doi.org/10.1016/j.cub.2014.09.014>.
 26. Gao, C., Zhuang, X., Cui, Y., Fu, X., He, Y., Zhao, Q., Zeng, Y., Shen, J., Luo, M., and Jiang, L. (2015). Dual roles of an Arabidopsis ESCRT component FREE1 in regulating vacuolar protein transport and autophagic degradation. *Proc. Natl. Acad. Sci. USA* 112, 1886–1891. <https://doi.org/10.1073/pnas.1421271112>.
 27. Kolb, C., Nagel, M.K., Kalinowska, K., Hagmann, J., Ichikawa, M., Anzenberger, F., Alkofer, A., Sato, M.H., Braun, P., and Isono, E. (2015). FYVE1 is essential for vacuole biogenesis and intracellular trafficking in Arabidopsis. *Plant Physiol.* 167, 1361–1373. <https://doi.org/10.1104/pp.114.253377>.
 28. Belda-Palazon, B., Rodriguez, L., Fernandez, M.A., Castillo, M.C., Anderson, E.M., Gao, C., Gonzalez-Guzman, M., Peirats-Llobet, M., Zhao, Q., De Winne, N., et al. (2016). FYVE1/FREE1 interacts with the PYL4 ABA receptor and mediates its delivery to the vacuolar degradation pathway. *Plant Cell* 28, 2291–2311. <https://doi.org/10.1105/tpc.16.00178>.
 29. Li, H., Li, Y., Zhao, Q., Li, T., Wei, J., Li, B., Shen, W., Yang, C., Zeng, Y., Rodriguez, P.L., et al. (2019). The plant ESCRT component FREE1 shuttles to the nucleus to attenuate abscisic acid signalling. *Nat. Plants* 5, 512–524. <https://doi.org/10.1038/s41477-019-0400-5>.
 30. Li, H., Li, T., Li, Y., Bai, H., Dai, Y., Liao, Y., Wei, J., Shen, W., Zheng, B., Zhang, Z., and Gao, C. (2023). The plant FYVE domain-containing protein FREE1 associates with microprocessor components to repress miRNA biogenesis. *EMBO Rep.* 24, e55037. <https://doi.org/10.15252/embr.202255037>.
 31. Hu, G., Katuwawala, A., Wang, K., Wu, Z., Ghadermarzi, S., Gao, J., and Kurgan, L. (2021). fIDPnn: Accurate intrinsic disorder prediction with putative propensities of disorder functions. *Nat. Commun.* 12, 4438. <https://doi.org/10.1038/s41467-021-24773-7>.
 32. Barberon, M., Dubeaux, G., Kolb, C., Isono, E., Zelazny, E., and Vert, G. (2014). Polarization of IRON-REGULATED TRANSPORTER 1 (IRT1) to the plant-soil interface plays crucial role in metal homeostasis. *Proc. Natl. Acad. Sci. USA* 111, 8293–8298. <https://doi.org/10.1073/pnas.1402262111>.
 33. Dobrenel, T., Mancera-Martinez, E., Forzani, C., Azzopardi, M., Davanture, M., Moreau, M., Schepetilnikov, M., Chicher, J., Langella, O., Zivy, M., et al. (2016). The arabidopsis TOR kinase specifically regulates the expression of nuclear genes coding for plastidic ribosomal proteins and the phosphorylation of the cytosolic ribosomal protein S6. *Front. Plant Sci.* 7, 1611. <https://doi.org/10.3389/fpls.2016.01611>.
 34. Xia, F.N., Zeng, B., Liu, H.S., Qi, H., Xie, L.J., Yu, L.J., Chen, Q.F., Li, J.F., Chen, Y.Q., Jiang, L., and Xiao, S. (2020). SINAT E3 ubiquitin ligases mediate FREE1 and VPS23A degradation to modulate abscisic acid signaling. *Plant Cell* 32, 3290–3310. <https://doi.org/10.1105/tpc.20.00267>.
 35. Zhang, T., Xiao, Z., Liu, C., Yang, C., Li, J., Li, H., Gao, C., and Shen, W. (2021). Autophagy mediates the degradation of plant ESCRT component FREE1 in response to iron deficiency. *Int. J. Mol. Sci.* 22, 8779. <https://doi.org/10.3390/ijms22168779>.
 36. Zeng, Y., Li, B., Huang, S., Li, H., Cao, W., Chen, Y., Liu, G., Li, Z., Yang, C., Feng, L., et al. (2023). The plant unique ESCRT component FREE1 regulates autophagosome closure. *Nat. Commun.* 14, 1768. <https://doi.org/10.1038/s41467-023-37185-6>.
 37. Kleine-Vehn, J., Leitner, J., Zwiewka, M., Sauer, M., Abas, L., Luschign, C., and Friml, J. (2008). Differential degradation of PIN2 auxin efflux carrier by retromer-dependent vacuolar targeting. *Proc. Natl. Acad. Sci. USA* 105, 17812–17817. <https://doi.org/10.1073/pnas.0808073105>.
 38. Spitzer, C., Reyes, F.C., Buono, R., Sliwinski, M.K., Haas, T.J., and Otegui, M.S. (2009). The ESCRT-Related CHMP1A and B proteins mediate multivesicular body sorting of auxin carriers in Arabidopsis and are required for plant development. *Plant Cell* 21, 749–766. <https://doi.org/10.1105/tpc.108.064865>.
 39. Katsiarimpa, A., Muñoz, A., Kalinowska, K., Uemura, T., Rojo, E., and Isono, E. (2014). The ESCRT-III-interacting deubiquitinating enzyme AMSH3 is essential for degradation of ubiquitinated membrane proteins in Arabidopsis thaliana. *Plant Cell Physiol.* 55, 727–736. <https://doi.org/10.1093/pcp/pcu019>.
 40. Watanabe, M., Balazadeh, S., Tohge, T., Erban, A., Givalisco, P., Kopka, J., Mueller-Roeber, B., Fernie, A.R., and Hoefgen, R. (2013). Comprehensive dissection of spatiotemporal metabolic shifts in primary, secondary, and lipid metabolism during developmental senescence in Arabidopsis. *Plant Physiol.* 162, 1290–1310. <https://doi.org/10.1104/pp.113.217380>.
 41. Zeng, Q., Araki, Y., and Noda, T. (2024). Pib2 is a cysteine sensor involved in TORC1 activation in *Saccharomyces cerevisiae*. *Cell Rep.* 43, 113599. <https://doi.org/10.1016/j.celrep.2023.113599>.
 42. Speiser, A., Silbermann, M., Dong, Y., Haberland, S., Uslu, V.V., Wang, S., Bangash, S.A.K., Reichelt, M., Meyer, A.J., Wirtz, M., and Hell, R. (2018). Sulfur partitioning between glutathione and protein synthesis determines plant growth. *Plant Physiol.* 177, 927–937. <https://doi.org/10.1104/pp.18.00421>.
 43. Caligaris, M., Nicastro, R., Hu, Z., Tripodi, F., Hummel, J.E., Pillet, B., Deprez, M.A., Winderickx, J., Rospert, S., Coccetti, P., et al. (2023). Snf1/AMPK fine-tunes TORC1 signaling in response to glucose starvation. *Elife* 12, e84319.
 44. Meng, D., Yang, Q., Wang, H., Melick, C.H., Navlani, R., Frank, A.R., and Jewell, J.L. (2020). Glutamine and asparagine activate mTORC1 independently of Rag GTPases. *J. Biol. Chem.* 295, 2890–2899. <https://doi.org/10.1074/jbc.AC119.011578>.
 45. Mülleder, M., Calvani, E., Alam, M.T., Wang, R.K., Eckerstorfer, F., Zelezniak, A., and Ralsler, M. (2016). Functional metabolomics describes the yeast biosynthetic regulome. *Cell* 167, 553–565.e12. <https://doi.org/10.1016/j.cell.2016.09.007>.
 46. Liu, K., Sutter, B.M., and Tu, B.P. (2021). Autophagy sustains glutamate and aspartate synthesis in *Saccharomyces cerevisiae* during nitrogen starvation. *Nat. Commun.* 12, 57. <https://doi.org/10.1038/s41467-020-20253-6>.
 47. Maeda, T., Wurgler-Murphy, S.M., and Saito, H. (1994). A two-component system that regulates an osmosensing MAP kinase cascade in yeast. *Nature* 369, 242–245. <https://doi.org/10.1038/369242a0>.
 48. Liu, Y., and Xiong, Y. (2021). Liquid culture system for efficient depletion of the endogenous nutrients in Arabidopsis seedlings. *STAR Protoc.* 2, 100922. <https://doi.org/10.1016/j.xpro.2021.100922>.
 49. Lenser, T., and Theißen, G. (2014). Floral dip transformation in *Lepidium campestre*. *Bio Protoc* 4, e1201. <https://doi.org/10.21769/bioprotoc.1201>.
 50. Nagel, M.K., Vogel, K., and Isono, E. (2019). Transient expression of ESCRT components in Arabidopsis root cell suspension culture-derived protoplasts. *Methods Mol. Biol.* 1998, 163–174. https://doi.org/10.1007/978-1-4939-9492-2_12.

STAR★METHODS

KEY RESOURCES TABLE

REAGENT or RESOURCE	SOURCE	IDENTIFIER
Antibodies		
Rabbit anti-phospho-RPS6A-Ser240	Agrisera	Cat#AS194302
Rabbit anti-RPS6A	Agrisera	Cat#AS194292
Rabbit anti-UGPase	Agrisera	Cat#AS05086
Rabbit anti-phospho S6K1/2	Agrisera	Cat#AS132664
Rabbit anti-S6K1/2	Agrisera	Cat#AS121855
Rabbit anti-HA	Agrisera	Cat#AS122220
Rabbit anti-FYVE1/FREE1	Agrisera	Cat#AS224702
Rabbit anti-PIN2	Agrisera	Cat#AS214697
Mouse anti-actin (C4)	Santa Cruz Biotechnology	Cat#SC-47778; RRID:AB_626632
Mouse anti-Ub(P4D1)	Cell Signaling Technology	Cat#3936, RRID:AB_331292
Mouse anti-GST (4C10)	BioLegends	Cat#901601
Sheep anti-Mouse IgG HRP-conjugated	Cytiva	Cat#NA931, RRID:AB_772210
Donkey anti-Rabbit IgG HRP Conjugated	Cytiva	Cat#NA934, RRID:AB_772206
Goat anti-Rabbit IgG HRP conjugated	Sigma-Aldrich	Cat#A0545, RRID:AB_257896
Bacterial and virus strains		
Escherichia coli Rosetta-gami B(DE3)	Novagen	Cat#71136
Chemicals, peptides, and recombinant proteins		
Torin 2	ChemScene	Cat#CS-0236
rapamycin	LC Laboratories	Cat#R-5000
Isopropyl β -D-1-thiogalactopyranoside (IPTG)	Nacalai	Cat#19742
M-MULV Reverse Transcriptase	New England Biolabs	Cat#M0253
Critical commercial assays		
NucleoSpin RNA Plant kit	Macherey-Nagel	Cat#740949
Experimental models: Organisms/strains		
<i>Arabidopsis</i> : Col-0	Lab Stock	N/A
<i>Arabidopsis</i> : 35Spro:3HA-RAPTOR1B	This study	N/A
<i>Arabidopsis</i> : fyve1-1	RIKEN	pst18264
<i>Arabidopsis</i> : fyve1-1, UBQ10pro:GFP-FYVE1	Kolb et al. ²⁷	N/A
<i>Arabidopsis</i> : 35Spro:3HA-FYVE1	This study	N/A
<i>Arabidopsis</i> : 35Spro:3HA-FYVE1 Δ 582-601	This study	N/A
Deposited data		
Raw and analyzed data	Mendeley Data	https://doi.org/10.17632/9vcy967fvd.1
Oligonucleotides		
Primers provided in Table S1		
Recombinant DNA		
Plasmids provided in Table S2		
Software and algorithms		
ImageJ	ImageJ	https://imagej.nih.gov/ij/
fIDPnn	Hu et al., 2021 ³¹	http://biomine.cs.vcu.edu/servers/fIDPnn/

EXPERIMENTAL MODEL AND STUDY PARTICIPANT DETAILS

Yeast strains and growth conditions

Yeast strains used in this study were in the S288C background and the genotypes are as follows. TM141 (*MATa leu2-Δ1 his3-Δ200 trp1-Δ63 ura3-52*)⁴⁷ and MH1059 (same as TM141 except *pib2::kanMX4*).²¹ Cells harboring plasmids were spotted on SD medium (1.7 g/L Yeast nitrogen base [Difco]), 5 g/L ammonium sulfate [supplemented with uracil, tryptophan, and histidine], 20.0 g/L glucose) plates with or without the indicated concentration of rapamycin and incubated at 30°C.

Plant material and growth conditions

All plant experiments were performed using *A. thaliana*. Arabidopsis seedlings were surface sterilized with 1% NaOCl, and kept at 4°C in the dark for 1–7 days, and grown on 1/2 Murashige & Skoog (MS) (2.15 g/L MS medium containing vitamins [Duchefa], 250 mg/L MES, pH 5.8) or MS with sucrose (4.3 g/L MS medium containing vitamins [Duchefa], 250 mg/L MES, 1% sucrose, pH 5.8) under long day (16 h light and 8 h dark) or continuous light conditions at 21°C for 5–10 days. For primary root growth assay, 1/4 MS with glucose (+N + G) and 1/4 MS without nitrogen but with glucose (-N + G) were prepared as previously described.⁴⁸ *fyve1-1* (RIKEN pst18264) and its complemented line with *UBQ10pro::GFP-FYVE1* were genotyped as previously described.²⁷ To generate *3HA-FYVE1*, *3HA-FYVE1ΔC*, and *3HA-RAPTOR1B* overexpressing lines, wild-type Col-0 was transformed by the floral dip method⁴⁹ with pMT20, pMT21, and pMT66, respectively.

METHOD DETAILS

Monitoring TOR kinase activity in seedlings

Arabidopsis seeds were sown in 6-well plates with 1 mL of 1/2 MS medium and grown for 6–7 days under long-day conditions (the liquid medium was replaced on day 3 or 4 and the day before harvest). The collected seedlings were immediately frozen in liquid nitrogen, ground with 2 × Laemmli sample buffer, and the samples were denatured for 4 min at 98°C. The samples were centrifuged at 15,000 × g for 2 min and the supernatant was subjected to immunoblotting using anti-RPS6A-P240 and anti-RPS6A antibodies.

Monitoring TOR kinase activity in protoplasts

Protoplasts derived from Arabidopsis root cell-derived cultures (Col-0) were transformed with the indicated plasmids using a polyethylene glycol-mediated method.⁵⁰ Subsequently, the protoplasts were suspended in MS + mannitol medium (MS containing vitamins and 0.4 M mannitol) and incubated overnight at 21°C in the dark. Transformed cell cultures were divided into two groups, one was treated with glutamine at a final concentration of 1 mM for 10 min. Trichloroacetic acid was added directly to the cultures at a final concentration of 7%. After incubation on ice for 1 h and centrifugation at 150 × g at 4°C for 3 min, cell precipitates were suspended in cold acetone and incubated at -25°C for 1–2 h. The cell suspensions were centrifuged at 24,000 × g for 30 min and the precipitates were washed once with cold acetone. The precipitates were then dried, suspended in urea buffer (25 mM Tris-HCl pH 6.8, 6 M urea, and 1% SDS), and briefly sonicated. Subsequently, 4 × Laemmli sample buffer was added to each sample and incubated at 65°C for 10 min. The samples were centrifuged at 15,000 × g for 2 min and the supernatant was subjected to immunoblotting.

GST-FYVE1 purification from *E. coli*

E. coli Rosetta-gami B(DE3) carrying pGEX4T-2-derived plasmids were cultivated in LB containing 15 μg/mL chloramphenicol and 100 μg/mL ampicillin at 37°C overnight. The overnight culture was then diluted in the same medium to an OD₆₀₀ of 0.35 and incubated for 1 h at 18°C before adding 0.5 mM of isopropyl-β-D-thiogalactoside. The culture was then incubated overnight at 18°C and the cells were collected, suspended in PBSN buffer (PBS +0.1% NP40, 1 mM phenylmethylsulfonyl fluoride, 40 μg/mL aprotinin, 10 μg/mL pepstatin A, 20 μg/mL leupeptin), and lysed by sonication. After centrifugation at 20,000 × g for 15 min, the supernatant was mixed with glutathione Sepharose 4B beads (Cytiva, Marlborough, MA, USA) and the mixture was rotated for 1 h at 4°C. The beads were washed three times with PBSN, and the precipitated proteins were eluted in an elution buffer (50 mM Tris-HCl [pH 8.0] and 10 mM reduced glutathione).

In vitro pull-down assay

7-day-old seedlings of *35Spro::3HA-Raptor1B* transgenic plants grown on MS with sucrose medium under continuous light or long-day conditions were quickly chilled in liquid nitrogen and grounded in a pull-down buffer (50 mM HEPES-KOH [pH 7.5], 120 mM NaCl, 1 mM EDTA, 0.1% Triton X-100, 1 mM phenylmethylsulfonyl fluoride, 40 μg/mL aprotinin, 10 μg/mL pepstatin A, and 20 μg/mL leupeptin) with liquid nitrogen. The extract was centrifuged at 20,000 × g for 15 min, and the supernatant was collected. The indicated amount of each amino acid was added to the supernatant along with purified GST-FYVE1 on Glutathione Sepharose beads (Cytiva, Durham, NC, USA), and the mixture was rotated for 1.5 h at 4°C. Subsequently, the beads were washed three times with the pull-down buffer containing the indicated amount of each amino acid, suspended in Laemmli sample dye, and boiled for 4 min. The supernatants were then subjected to immunoblotting.

qRT-PCR

Seedlings frozen in liquid nitrogen were extracted using a TissueLyser (Qiagen) with 1.2 mm diameter glass beads. Total RNA was isolated using the NucleoSpin RNA Plant Kit (Macherey-Nagel, Düren, Germany), followed by cDNA synthesis using M-MULV Reverse Transcriptase

(New England Biolabs, Beverly, MA, USA). The cDNA was analyzed by RT-PCR using gene-specific primers oMH73/oMH74 for *FYVE1* and GAPDH fw/GAPDH rv for *GAPDH*.

QUANTIFICATION AND STATISTICAL ANALYSIS

Statistical analyses were performed using Microsoft Excel software. Details of statistical analyses are included in the corresponding figure legends. All the data are presented as the mean \pm SD. Student's two-tailed t-test was used to evaluate group differences. *p*-value of less than 0.05 was considered to indicate statistical significance (**p* < 0.05; ***p* < 0.01; ****p* < 0.001). *p*-value >0.05 was considered not significant and was denoted by "n.s".

No specific methods were used to test whether the data met the assumptions of the statistical approach.